JOURNAL OF MATERIALS SCIENCE 23 (1988) 1605–1609

Microstructure and mechanical properties of Al_2O_3–Cr_2O_3–ZrO_2 composites

TADAHISA ARAHORI
Technical Research Laboratories, Sumitomo Metal Industries Ltd, 16 Sunayama, Hasaki, Ibaraki 314-02 Amagasaki 660, Japan

E. DOW WHITNEY
Department of Materials Science and Engineering, University of Florida, Gainesville, Florida, 32611, USA

Al_2O_3 is a popular ceramic and has been used widely in many applications and studied in many aspects. On the other hand, zirconia-toughened alumina (ZTA) is a desirable material for engineering ceramics because of its high hardness, high wear resistance and high toughness. In the present research, Al_2O_3–Cr_2O_3–ZrO_2 composites were produced by hot-pressing in order to harden the Al_2O_3 matrix in ZTA. Its microstructure and mechanical properties were studied by SEM, ESCA, XRD, Vickers hardness and bending strength test. It was found that addition of ZrO_2 inhibited the grain growth of Al_2O_3–Cr_2O_3 and the grain growth of ZrO_2 proceeded with increasing amounts of ZrO_2 in the Al_2O_3–Cr_2O_3–ZrO_2 composite. The formation of solid solution Al_2O_3–Cr_2O_3 was also confirmed by XRD, and monoclinic ZrO_2 increased on addition of Cr_2O_3. Maximum hardness was at Al_2O_3–10 wt% Cr_2O_3 with 10 vol% ZrO_2 and a stress-induced transformation was confirmed on the fracture surface of the specimen after the bending test.

1. Introduction

It is well known that the monoclinic phase of ZrO_2 is stable below 1200° C, the tetragonal phase is stable between 1200 and 2372° C, and the cubic phase is stable above 2372° C [1]. The transformation of monoclinic to tetragonal is reversible and is accompanied by a volume change. Therefore, cubic ZrO_2 stabilized with CaO, MgO, Y_2O_3 etc. has been used as refractories. However, since partially stabilized ZrO_2 (PSZ), which partially consists of tetragonal phase and is very tough, was reported by Garvie *et al.* [2], it has become a desirable material for use as engineering ceramics.

Zirconia-toughened alumina (ZTA) is also a desirable material for engineering ceramics because of its high hardness, high wear resistance and high toughness. In ZTA, microstructure and mechanical properties have been studied by Lange and co-workers [3, 4] and Claussen [5] etc. Al_2O_3 is a popular ceramic and has been used widely for many applications and studied in many aspects, especially the grain-size influence on the mechanical properties of the ceramic body, so that MgO, TiO_2, Cr_2O_3 are used as grain growth inhibitors in Al_2O_3 ceramics. It has also been reported that Cr_2O_3 produces a solid solution with Al_2O_3 which improves the mechanical properties of the latter [6].

In the present research, Al_2O_3–Cr_2O_3–ZrO_2 composites were produced in order to harden the Al_2O_3 matrix in ZTA and the microstructure and mechanical properties of this composite were studied by scanning electron microscopy (SEM), electron spectroscopy for chemical analysis (ESCA), X-ray diffraction (XRD), Vickers hardness test and bending strength test.

2. Experimental details

2.1. Materials

Powdered materials were prepared from Al_2O_3 (average particle diameter 0.3 μm: Fisher, Pittsburgh) and $Cr(NO_3)_3 \cdot 9H_2O$ (Fisher, Pittsburgh) and $ZrOCl_2 \cdot 8H_2O$ (Aldrich, Milwaukee). Al_2O_3 powder and soluble $Cr(NO_3)_3 \cdot 9H_2O$ and $ZrOCl_2 \cdot 8H_2O$ in water were mixed and precipitated with NaOH solution while stirring. The mixtures were filtered, washed with water, dried and then calcined and ground in a ball milling jar. Specimens of several compositions were hot-pressed in graphite dies in a nitrogen atmosphere at 1500° C for 2 h under a pressure of 20.7 MPa. Sintered specimens were ground and annealed at 1350° C.

2.2. Measurements

The microstructure of specimens was observed by optical microscopy and SEM. The states of aluminium, chromium and zirconium were analysed by ESCA (VG: ESCA 3MKII).

The crystal phases of ZrO_2 were identified by XRD. It has already been shown that the sum of the integral intensity of monoclinic (1 1 1), ($\bar{1}$ 1 1) and tetragonal (1 1 1) and cubic (1 1 1) in ZrO_2 is constant, and also that of tetragonal (0 0 4), (4 0 0) and cubic (4 0 0) is constant [7]. Miller *et al.* [8] gave equations for calculating the molecular ratio of monoclinic, tetragonal and cubic phase in ZrO_2 by XRD. In the present research, the crystal phase ratio in ZrO_2 was measured

0022–2461/88 $03.00 + .12

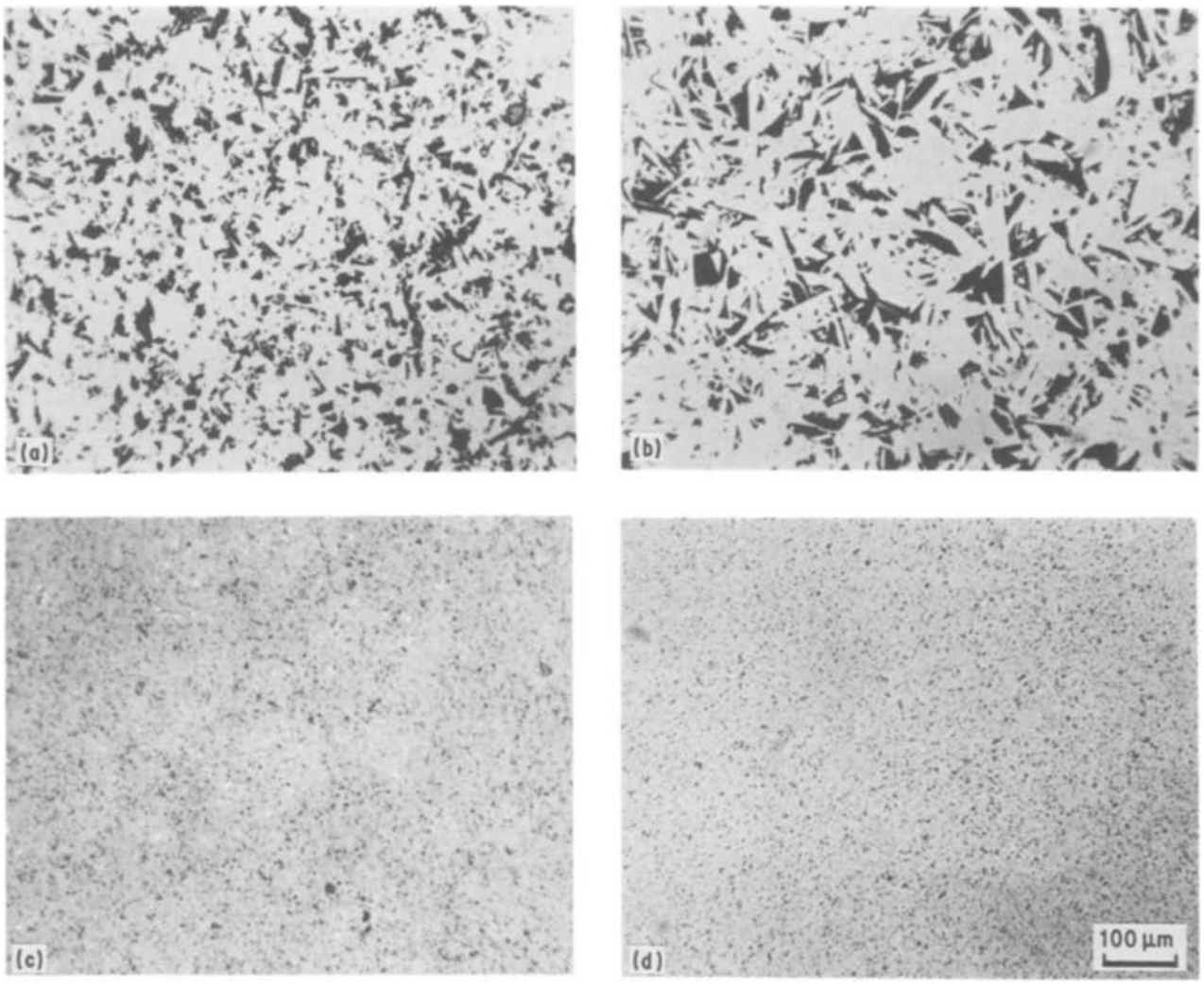

Figure 1 Microstructure of a polished surface of Al_2O_3–Cr_2O_3–ZrO_2 composites seen by optical microscopy. (a) Al_2O_3–5 wt % Cr_2O_3, (b) Al_2O_3–10 wt % Cr_2O_3, (c) (Al_2O_3–5 wt % Cr_2O_3)–10 vol % ZrO_2, (d) (Al_2O_3–10 wt % Cr_2O_3)–10 vol % ZrO_2.

by following the former method. On the other hand, the lattice constants of Al_2O_3 were measured in order to investigate the Al_2O_3–Cr_2O_3 solid solution. In the measurement of lattice constants, the Nelson–Riley extrapolation function [9] and the method of least squares were employed and then a and c were calculated.

Hardness, fracture toughness and bending strength as mechanical properties were measured on Al_2O_3–Cr_2O_3–ZrO_2 composites. Vickers hardness was measured and specimens were loaded at 10 kg for 15 sec. Fracture toughness was given by measuring the length of the cracks from the Vickers indentation and by using the following experimental equation [10],

$$K_{IC}/H\,a^{1/2} = 0.203(c/a)^{-3/2} \quad (1)$$

where H is the Vickers hardness, a the length of the indentation and c the length of the crack. Strength was measured by three-point bending. The size of the specimen for this test was 3 mm × 4 mm × 40 mm and the span length was 30 mm.

3. Results

The microstructure of a polished surface of Al_2O_3–Cr_2O_3–ZrO_2 composites was observed by optical microscopy as shown in Fig. 1. In Al_2O_3–Cr_2O_3 composite, wedge-shaped crystals were observed and grains grew with increasing Cr_2O_3 content. On the other hand, the texture was very fine and homogeneous in the composition, including ZrO_2.

Fig. 2 shows scanning electron micrographs of Al_2O_3–Cr_2O_3–ZrO_2 composites. ZrO_2 particles were dispersed homogeneously in four-grain junctions of Al_2O_3 particles in the specimen including 10 vol% ZrO_2. It is indicated that the fine ZrO_2 particles were included in Al_2O_3 grains on the grain growth of the Al_2O_3 particle, and ZrO_2 grains were included in the interface of Al_2O_3 grains in the specimen including 25 vol % ZrO_2. Furthermore, Al_2O_3 and ZrO_2 grains grew greatly in 40 vol % ZrO_2. The average grain sizes of ZrO_2 particles were 0.5 μm in 10 vol % ZrO_2, 1.0 μm in 25 vol % ZrO_2 and 2.1 μm in 40 vol % ZrO_2.

The results analysed by ESCA for Al_2O_3–Cr_2O_3–ZrO_2 composite are given in Fig. 3. It was confirmed that aluminium is present as Al_2O_3, chromium as Cr_2O_3 and zirconium as ZrO_2 by analysing Al2P, Cr2P3/2, Zr3d, and sodium and nitride were not detected.

ZrO_2 phases of hot-pressed Al_2O_3–Cr_2O_3–10 vol% ZrO_2 composites were identified by XRD. As cubic phase (4 0 0) was not detected clearly, it is supposed that these composites consist of monoclinic and tetragonal without the cubic phase in ZrO_2. The monoclinic ratio calculated from monoclinic (1 1 1), (1 1 $\bar{1}$) and

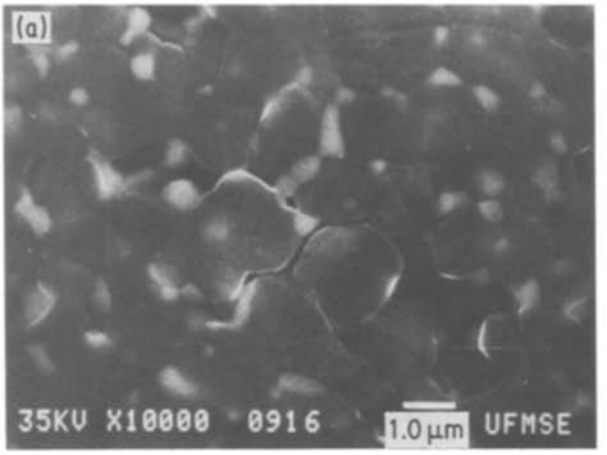

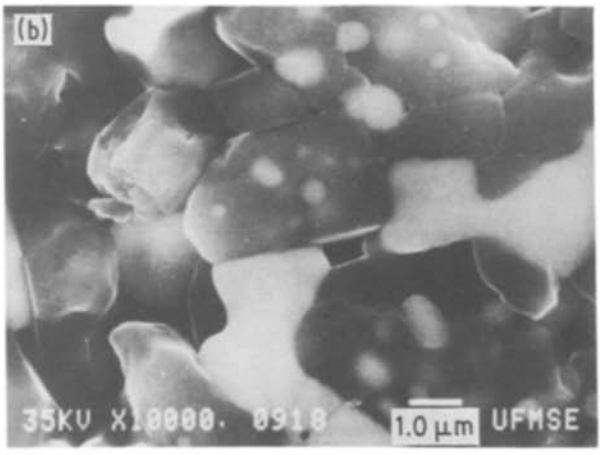

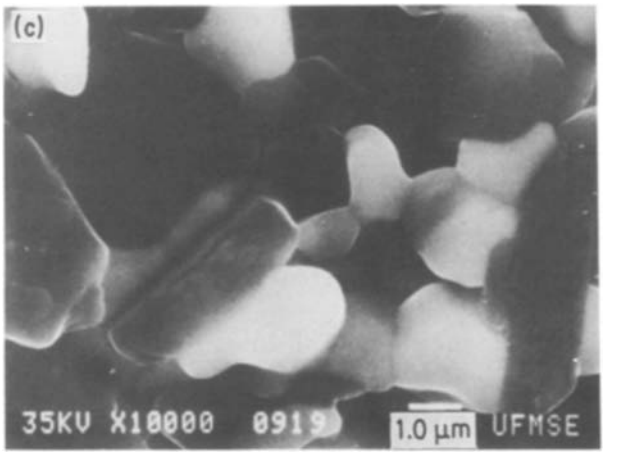

Figure 2 Scanning electron micrographs of (a) (Al_2O_3–10 wt % Cr_2O_3)–10 vol % ZrO_2, (b) (Al_2O_3–10 wt % Cr_2O_3)–25 vol % ZrO_2, (c) (Al_2O_3–10 wt % Cr_2O_3)–40 vol % ZrO_2 composites.

tetragonal (1 1 1) is indicated in Fig. 4. It is obvious that the monoclinic phase increases with increasing amount of Cr_2O_3. Fig. 5 shows the changes in the lattice constants of Al_2O_3 in Al_2O_3–Cr_2O_3–ZrO_2 composite. The values of a_0 and c_0 increase with increasing amount of Cr_2O_3. This result indicates that Al_2O_3 and Cr_2O_3 formed a solid solution.

Fig. 6 shows the dependence of Vickers hardness on the Cr_2O_3 content in Al_2O_3–Cr_2O_3–ZrO_2 composite. The hardness was maximum at the composition Al_2O_3–10 wt % Cr_2O_3 in Al_2O_3–Cr_2O_3–10 vol % ZrO_2 composites. Fracture toughness (K_{IC}), measured by Vickers indentation in Al_2O_3–Cr_2O_3–10 vol % ZrO_2 composites, is indicated in Fig. 7: the fracture toughness increased with increasing amount of Cr_2O_3 and saturated at the composition Al_2O_3–10 wt % Cr_2O_3 in Al_2O_3–Cr_2O_3–10 vol % ZrO_2 composites. In addition, the bending strength of (Al_2O_3–10 vol % Cr_2O_3)–10 vol % ZrO_2 composite was 556 MPa.

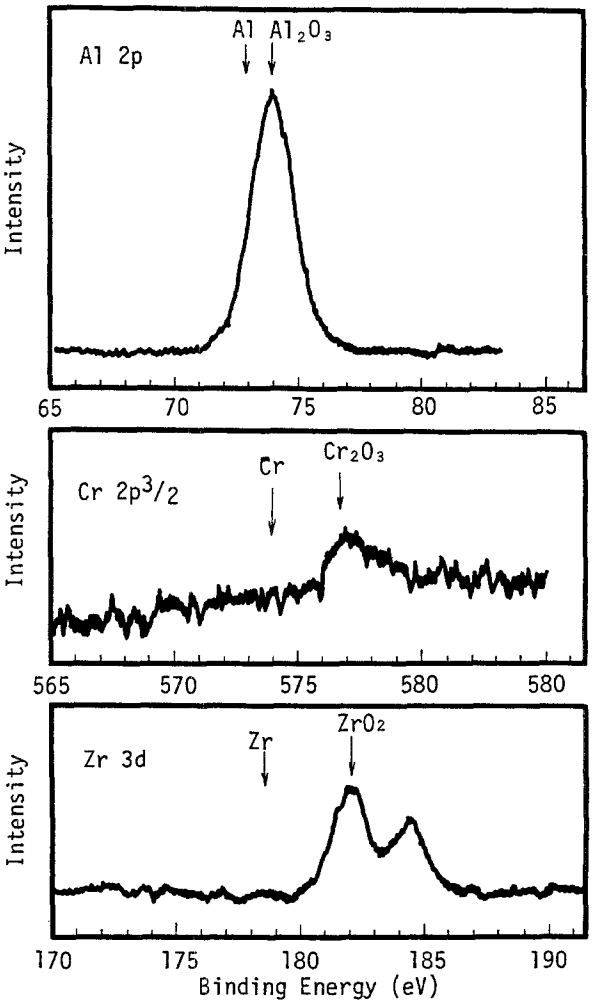

Figure 3 ESCA patterns of (Al_2O_3–10 wt % Cr_2O_3)–10 vol % ZrO_2 composite.

4. Discussion

As Al_2O_3 is the main component in Al_2O_3–Cr_2O_3–ZrO_2 composites, its properties influence the properties of the body as a whole. It is especially important to inhibit grain growth and to distribute fine grains

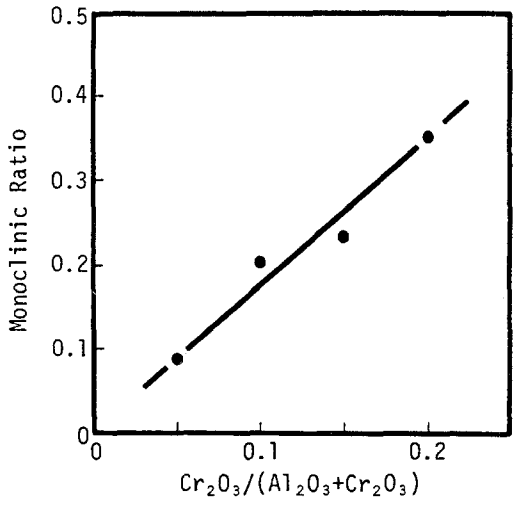

Figure 4 Monoclinic phase ratio of ZrO_2 in (Al_2O_3–Cr_2O_3)–10 vol % ZrO_2 composites obtained by X-ray diffraction.

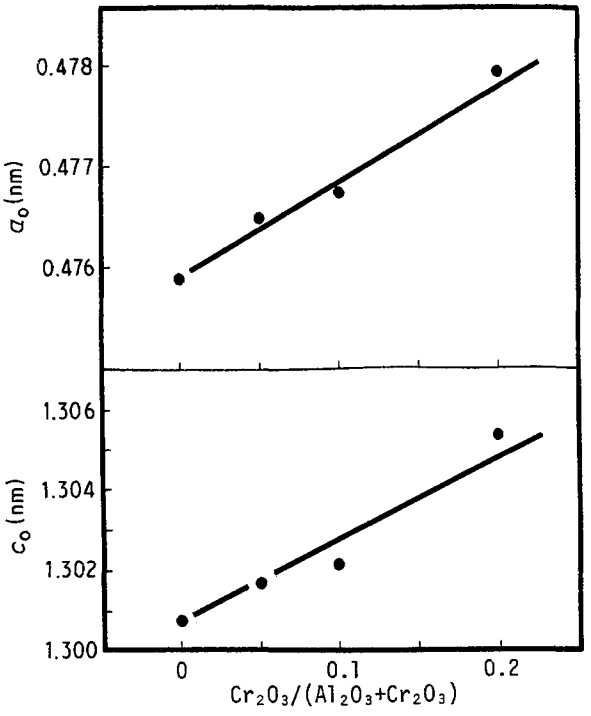

Figure 5 Lattice constants of Al_2O_3 in (Al_2O_3–Cr_2O_3)–10 vol % ZrO_2 composites.

homogeneously. From observation of the microstructure in Fig. 1 it is indicated that ZrO_2 is very effective in inhibiting grain growth of the Al_2O_3–Cr_2O_3 matrix. Therefore, addition of small amounts of Cr_2O_3 is effective as a grain growth inhibitor; however, it is not effective in these compositions. On the other hand, Lange and Hirlinger [11] investigated the relationship between the amount of ZrO_2 and grain growth in Al_2O_3–ZrO_2 composites. In his results, although ZrO_2 is present as less than 5 vol %, it does not contribute as a grain growth inhibitor for Al_2O_3, and abnormal grain growth is also observed. More than 5 vol % ZrO_2 does inhibit grain growth. It is important for ZrO_2 to be in the four-grain junctions of Al_2O_3 grains in order to produce a fine microstructure. In the present compositions, ZrO_2 inhibits the grain growth of

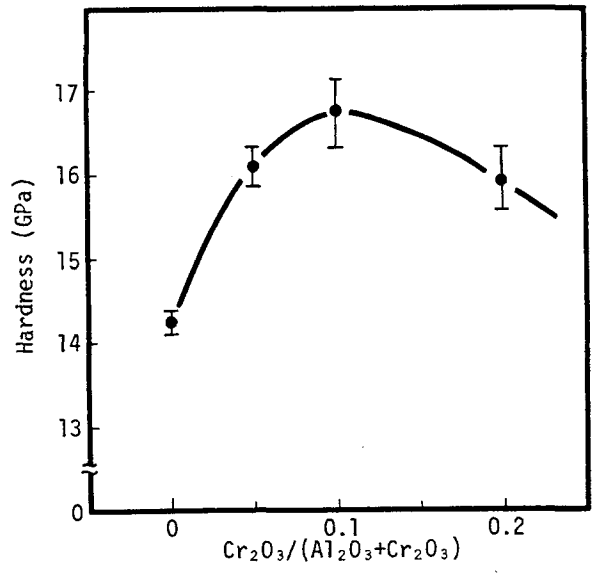

Figure 6 Vickers hardness of (Al_2O_3–Cr_2O_3)–10 vol % ZrO_2 composites.

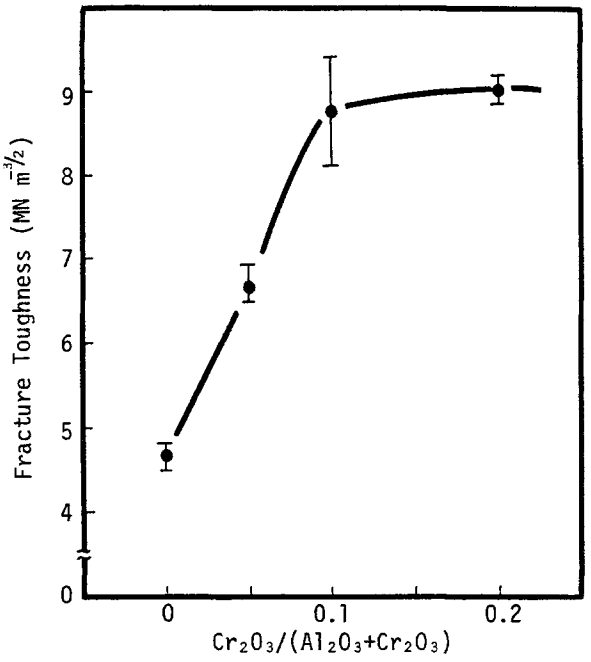

Figure 7 Fracture toughness of (Al_2O_3–Cr_2O_3)–10 vol % ZrO_2 composites.

Al_2O_3–Cr_2O_3, as shown in Fig. 1 because more than 5 vol % ZrO_2 is present in the Al_2O_3–Cr_2O_3–ZrO_2 composite. However, in part of the heterogeneous distribution of ZrO_2 grains, an abnormal grain growth of Al_2O_3–Cr_2O_3 was observed, as shown in Fig. 8. This phenomenon suggests that the homogeneous distribution of ZrO_2 is an important factor.

The grain size of ZrO_2 changes with its amount in the composite and it enlarges with increasing amount of ZrO_2 as shown in Fig. 2. It was observed that ZrO_2 grains, which existed between Al_2O_3 grains, grew and jointed with their neighbours and then each became a large grain. It is thought the reason that the influence of Al_2O_3–Cr_2O_3 grains on ZrO_2 grains becomes less with increasing amount of ZrO_2 in the Al_2O_3–Cr_2O_3–ZrO_2 composite is that there is a reciprocal action between Al_2O_3–Cr_2O_3 grains and ZrO_2 grains. Green also reported this phenomenon in ZTA [12].

It is obvious that Al_2O_3 forms a solid solution with Cr_2O_3 in Al_2O_3–Cr_2O_3–ZrO_2 composite as shown in Fig. 5. Rossi and Lawrence [13] also measured the

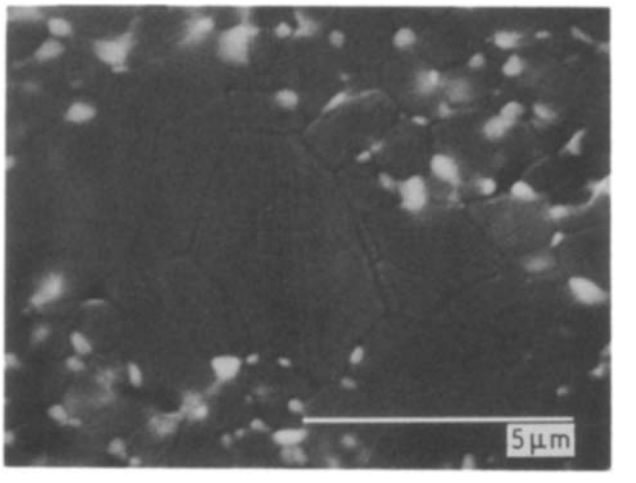

Figure 8 Scanning electron micrograph of the luck area of ZrO_2 in (Al_2O_3–10 wt % Cr_2O_3)–10 vol % ZrO_2 composite.

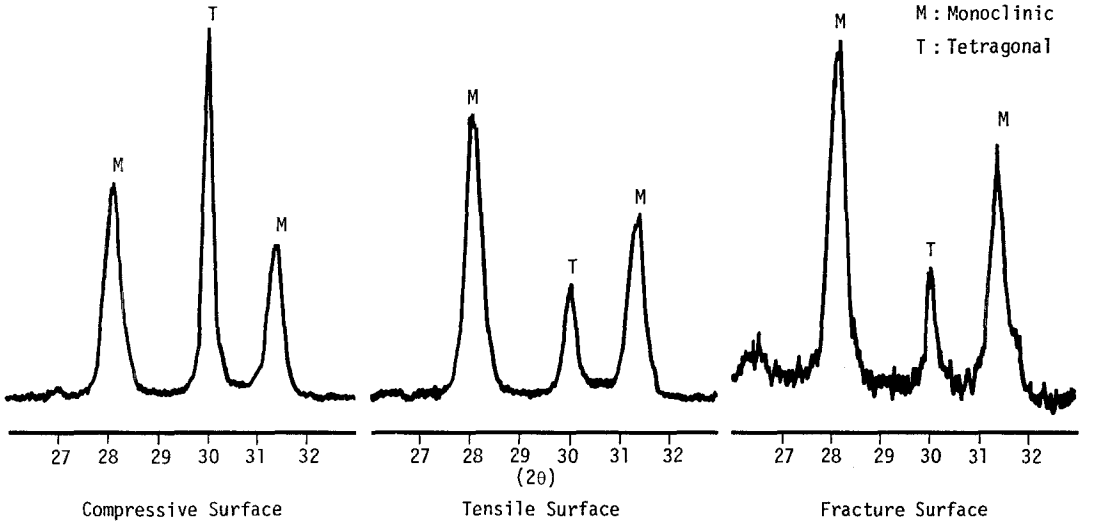

Figure 9 X-ray diffraction patterns of (Al_2O_3–10 wt % Cr_2O_3)–10 vol % ZrO_2 composite after the bending test.

lattice constant of Al_2O_3 with Cr_2O_3 and confirmed the solid solution as Al_2O_3–Cr_2O_3. On the other hand, Jayaratna *et al.* [14] reported that the solubility of Cr_2O_3 in ZrO_2 was 0.7 mol % at 1450° C. Therefore, Cr_2O_3 may also slightly dissolve in ZrO_2 in Al_2O_3–Cr_2O_3–ZrO_2 composite.

Bradt [6] concluded that the hardness of Al_2O_3–Cr_2O_3 composite increased with increasing Cr_2O_3 content. Ghate *et al.* [15] also measured the hardness of Al_2O_3–Cr_2O_3 composites and concluded that the maximum hardness was at 10 mol % Cr_2O_3. This result is similar to that in Fig. 6. In any case, the addition of Cr_2O_3 to Al_2O_3 is effective in improving the mechanical properties and it was surmised that solid solution hardening might be a grain-boundary effect.

It is known that partially stabilized ZrO_2 has a stress-induced transformation from tetragonal to monoclinic phase which improves the properties of fracture toughness and strength by a volume change of ZrO_2. Tetragonal ZrO_2 exists in our specimens, so it is presumed that this transformation occurs to strengthen and improve fracture toughness in the Al_2O_3–Cr_2O_3–ZrO_2 composite. Besides, although the tetragonal phase decreased with increasing Cr_2O_3 content, fracture toughness increased. It is considered that microcracks, which were produced on transformation of tetragonal to monoclinic ZrO_2 in the sintering process, exist in the specimens and thus may also contribute to high fracture toughness. The ZrO_2 phases of the specimen after the bending test were identified by X-ray diffraction as shown in Fig. 9. It was certified that the stress-induced transformation proceeded on the fracture surface. In addition, the transformation on the tensile (lower) surface proceeded more than on the compressive (upper) surface. It is thus assumed that the constraint force of the Al_2O_3–Cr_2O_3 matrix against the ZrO_2 grains was released by the tensile stress [16].

5. Conclusions

1. The addition of ZrO_2 inhibited the grain growth of Al_2O_3–Cr_2O_3 and the grain growth of ZrO_2 proceeded with increasing amount of ZrO_2 in the Al_2O_3–ZrO_2 composite. No compounds other than Al_2O_3, Cr_2O_3 and ZrO_2 were found in the Al_2O_3–Cr_2O_3–ZrO_2 composite using ESCA measurement.

2. The formation of a solid solution of Al_2O_3–Cr_2O_3 was confirmed by measuring the lattice constants of Al_2O_3, and the monoclinic phase of ZrO_2 in Al_2O_3–Cr_2O_3–ZrO_2 composite increased with the addition of Cr_2O_3.

3. The hardness was maximum at the composition of Al_2O_3–10 wt % Cr_2O_3 and the fracture toughness increased with increasing amount of Cr_2O_3 in the Al_2O_3–Cr_2O_3–10 vol % ZrO_2 composites.

4. The stress-induced transformation in Al_2O_3–Cr_2O_3–ZrO_2 composite was confirmed on the fracture surface of the specimen after the bending test by XRD and that it proceeded more on the tensile surface than on the compressive surface.

References

1. E. M. LEVIN and H. F. McMURDIE, "Phase Diagrams for Ceramists" (American Ceramic Society, Columbus, 1975).
2. R. C. GARVIE, R. H. HANNINK and R. T. PASCOE, *Nature* **258** (1975) 703.
3. F. F. LANGE and D. J. GREEN, "Advances in Ceramics", Vol. 3 (American Ceramic Society, Columbus, 1981) pp. 217-25.
4. F. F. LANGE and M. M. HIRLINGER, *J. Amer. Ceram. Soc.* **67** (1984) 164.
5. N. CLAUSSEN, *ibid.* **59** (1976) 49.
6. R. C. BRADT, *ibid.* **50** (1967) 54.
7. R. C. GARVIE and P. S. NICHOLSON, *ibid.* **55** (1972) 303.
8. R. A. MILLER, J. L. SMIALEK and R. G. GARLICK, "Advances in Ceramics", Vol. 3 (American Ceramic Society, Columbus, 1981) pp. 241-53.
9. K. NIIHARA, *Ceramics* **20** (1985) 12.
10. B. D. CULLITY, "Elements of X-ray Diffraction" (Addison-Wesley, Reading, 1956).
11. F. F. LANGE and M. M. HIRLINGER, *J. Amer. Ceram. Soc.* **67** (1984) 164.
12. D. J. GREEN, *ibid.* **65** (1982) 610.
13. L. R. ROSSI and W. G. LAWRENCE, *ibid.* **53** (1970) 604.
14. M. JAYARATNA, M. YOSHIMURA and S. SOMIYA, *J. Mater. Sci.* **21** (1986) 591.
15. B. B. GHATE, W. C. SMITH, C. H. KIM, D. P. H. HASSELMAN and G. E. KANE, *Ceram. Bull.* **54** (1975) 210.
16. T. ARAHORI, N. IWAMOTO and N. UMESAKI, *J. Ceram. Soc. Jpn* **94** (1986) 742.

Received 27 April
and accepted 6 July 1987